https://doi.org/10.5194/angeo-2020-71
Preprint. Discussion started: 23 October 2020

Annales Geophysicae Discussions
Open Access
EGU

Modelling the residual mean meridional circulation at different stages of stratospheric warming events

Andrey V. Koval[1,2], Anna N. Bakhareva[1], Ksenia A. Didenko[1,2], Tatiana S. Ermakova[1,2], Nikolai M. Gavrilov[1], Alexander I. Pogoreltsev[1,2], Olga N. Toptunova[1,2], Anton S. Zarubin[1]

[1]Atmospheric Physics Department, Saint-Petersburg State University, Saint-Petersburg, 198504, Russia
[2]Department of Meteorological Forecasts, Russian State Hydrometeorological University, Saint-Petersburg, Russia

Correspondence to: Andrey V. Koval (a.v.koval@spbu.ru)

Abstract. Ensemble simulation of the general atmospheric circulation of the middle and upper atmosphere up to the lower thermosphere is performed using the 3-D nonlinear mechanistic numerical model MUAM. Residual mean meridional circulation (RMC) in terms of the Transformed Eulerian Mean is calculated for the boreal winter and changes in its vertical and meridional velocity components during different phases of simulated composite stratospheric warming (SW) events are studied. The simulation results show general decrease in RMC velocity components up to 30% during and after SW in the mesosphere and lower thermosphere of the Northern Hemisphere. There are also increases in the downward and northward velocities at altitudes 50-70 km at the northern high latitudes. Associated changes in adiabatic heating/cooling rates can contribute to heating the stratosphere and cooling the mesosphere during the composite SW. The changes in the transport of conservative species (like ozone) during SWs are estimated. Weakening of ozone fluxes at the middle latitudes of the Northern Hemisphere may reach 30% during SWs and 30 – 40% after the events at the altitudes of stratospheric maximum of ozone concentration. Such statistically confident simulations of RMC reactions on SWs at altitudes up to the lower thermosphere are performed for the first time. The study of the residual meridional circulation is useful for effective analysis of wave impacts on the mean flow and for diagnostics of the transport of atmospheric gas species in the atmosphere.

Keywords: residual circulation; transformed Eulerian mean; sudden stratospheric warming; numerical modelling

1. Introduction

The circulating transport of trace gases in the middle and upper atmosphere affects the overall distribution of ozone and other atmospheric gas components. The main mechanism for the global transport of trace gases (e.g., Fishman and Crutzen, 1978) between the stratosphere and troposphere is the Brewer-Dobson meridional circulation (Dobson et al., 1929; Dobson, 1956; Brewer, 1949). This is in a general sense, global mass transfer, in which tropospheric air enters the stratosphere in the tropics, then travels to the poles and sinks down in middle and high latitudes. At the mesospheric heights, it is essential to consider the mesospheric meridional circulation, implying the mass transfer from the summer hemisphere to the winter one.

In the last decades, there has been a surge of interest in the study of the Brewer-Dobson circulation, which is associated mainly with the active development of general circulation models (e.g., Pawson et al., 2000; Gerber et al., 2012 and references therein), chemical-climatic models (Eyring et al., 2005; SPARC CCMVal, 2010). A large number of studies are also devoted to reanalysis data processing and interpretation of observed atmospheric processes (Iwasaki et al., 2009; Sevior et al., 2012, etc.).

It is well known, that atmospheric waves can substantially modify the mean Eulerian meridional circulation, i.e. zonal averaging of the mean meridional and vertical flows is ineffective for analyzing global transport of atmospheric species. In the momentum and energy equations, the wave sources of momentum and heat are partly compensated by advective momentum and heat fluxes (e.g., Charney and Drazin, 1961). With the Eulerian approach, similar compensation of wave and mean mass fluxes occurs also in the continuity equation for long-lived gas components. These features do not allow one to

https://doi.org/10.5194/angeo-2020-71
Preprint. Discussion started: 23 October 2020

isolate the wave action from that of the mean flow. In order to overcome this disadvantage, it is essential to use alternative approaches to the analysis of the zonal-mean circulation, one of which is the calculation of the transformed Eulerian mean (TEM) circulation (e.g., Andrews and McIntyre, 1976) that are used in the present study. This approach provides effective diagnostics of wave impacts on the mean flow, and also, provides the ability to calculate the meridional transport of conservative gas species. This method leads to the consideration of the so-called mean residual meridional circulation (RMC), which is a combination of eddy and advective mean transport. RMC estimates residual parts of the mean flow, which not compensated by the divergence of the wave-induced eddy momentum and heat fluxes (e.g., Shepherd, 2007). In its traditional form, the RMC is two-dimensional and formulas describing it include zonally averaged values of atmospheric parameters, (e.g., Holton, 2004). However, the underlying mechanism of wave excitation is three-dimensional, which requires the use of 3-dimensional numerical modelling for the correct reproduction of RMC properties.

Sudden stratospheric warming (SSW) event is one of the most dramatic dynamical processes appearing at high latitudes of the northern middle atmosphere. The zonal-mean meridional thermal gradient, usually directed towards the equator in winter, reverse its direction in the stratosphere during SSWs to the opposite. In the case of a major SSW, the eastward zonal velocity in the polar stratosphere also reverses direction, while in the case of a minor SSW, only a weakening of the zonal wind velocity is observed (e.g., Holton, 2004; McIntyre, 1982). SSW events can substantially affect the dynamics and energetics at different atmospheric layers (Siskind et al., 2010; Fuller-Rowell et al., 2010; Funke et al., 2010; Liu et al., 2011; Yuan et ql., 2012; Sun and Robinson, 2009; Nath et al., 2016). Changes in meridional circulation during different phases of SSW event were recently studied by Tao et al. (2017), de la Camara et al. (2018),

Koval et al. (2019) simulated the mean meridional circulation and its changes during SSW events. They showed that the global-scale Eulerian mean meridional circulation in the middle atmosphere might significantly alter at different stages of stratospheric warming during the northern winter season, which can be essential for the transport of conservative gas species in the middle and upper atmosphere. However, as stated above, the net transport of gas species should include contribution of wave eddy effects and requires RMC calculating.

In this study, we extended simulations by Koval et al. (2019) to calculate the RMC components based on the simulated wind and temperature fields for the boreal winter season. Using the atmospheric circulation model MUAM, responses of RMC structure on composite SSW events up to the altitudes of the lower thermosphere are studied for the first time. Statistically confident ensemble results for altitudes up to of the mesosphere and lower thermosphere (MLT) are obtained. The study of RMC made it also possible to estimate the total circulating transport of conservative gas species (like ozone) in the middle and upper atmosphere.

2. Methodology

In order to study the changes in the RMC at time intervals before, during and after simulated SSW events, the middle and upper atmosphere model (MUAM) is used to describe general circulation at altitudes up to the lower thermosphere (Pogoreltsev et al., 2007). It is a 3-D nonlinear mechanistic numerical model. The horizontal grid steps of the model are 5.625° in longitude and 5° in latitude. The vertical grid of the model is log-isobaric coordinate $z = -H * ln (p_0/p)$, where p_0 is the surface pressure and H = 7 km is the pressure scale height. The MUAM is based on a standard set of primitive equations in the spherical coordinates used in the Cologne Model of the Middle Atmosphere-Leipzig Institute for Meteorology (COMMA-LIM) described by Fröhlich et al. (2003). A detailed description of the MUAM and processes implemented into the model are presented by Gavrilov et al. (2005) and Pogoreltsev et al. (2007). Details of the numerical experiments and used methods for determining the dates of SSW onset are similar to those described by Koval et al. (2019).

According to recent knowledge, an important driving force of the atmospheric meridional circulation are planetary-scale wave disturbances (e.g., Haynes et al., 1991; Holton et al., 1995). The MUAM model reproduces spectra of global-scale and

https://doi.org/10.5194/angeo-2020-71
Preprint. Discussion started: 23 October 2020

mesoscale wave disturbances (Pogoreltsev et al., 2014, Gavrilov et al., 2015; 2018) as well as atmospheric tides (Suvorova and Pogoreltsev, 2011). The amplitudes of stationary planetary waves (SPWs) at the lower boundary are calculated from the geopotential height distributions in the lower atmosphere obtained from reanalysis of meteorological information UK Met Office (UKMO, Swinbank and O'Neill, 1994). In addition, the MUAM includes a parameterization of the westward travelling atmospheric normal modes with zonal wave numbers m = 1 - 3 and periods from 2 to 16 days (Pogoreltsev et al., 2009). The model also includes parameterizations of the dynamic and thermal effects of stationary orographic gravity waves developed by Gavrilov and Koval (2013) and of nonorographic gravity waves (GWs), which is similar to those developed by Lindzen (1981) and Yigit and Medvedev (2009). Estimations by Pogoreltsev et al. (2007) and Gavrilov el al. (2015) showed that the MUAM satisfactorily reproduces the structure of atmospheric circulation up to altitudes of the lower thermosphere.

To improve the statistical significance and smooth out the interannual variability in the MUAM, an ensemble of 19 model runs was obtained, containing major or minor SSW events during model runs for January-February conditions. Different MUAM runs correspond to different phases of vacillations between the mean wind and SPWs in the middle atmosphere. These phases in the MUAM are controlled by changing of the inclusion date of daily variations in the solar heating and generation of normal atmospheric modes in different ensemble members of model runs (Pogoreltsev et al., 2007, 2009).

The model dates or simulated SSWs were obtained using the definition by Charlton and Polvani (2007). However zonal wind reversals at every MUAM run were detected not only at pressure level of 10 hPa (near 30 km altitude), but also at higher altitudes up to 50 km (Savenkova et al., 2017; Gavrilov et al., 2018). To differentiate these phenomena from traditionally considered SSWs near 10 hPa pressure level, we call them simply as “stratospheric warmings” (SWs). Types of SW events may be different for different model runs. Examples of temperature and wind variations during SW events simulated with the MUAM runs one can see in Figure 1 of the papers by Koval et al. (2019) and Gavrilov et al. (2018).

The changes of thermodynamic fields in different MUAM runs could be considered as variability corresponding to different phases of stratospheric vacillations in different years. For each simulated SW event, its onset date was determined and three 11-day consecutive intervals were selected before, during and after the SW. After averaging over all simulated SWs, this approach allowed us to obtain average characteristics for a composite SW event statistically relevant to the SW climatology obtained by analyzing processing multi-year reanalysis data and described, for instance, by Savenkova et al. (2017).

3. Calculating the residual mean meridional circulation

Residual circulation in this study is understood in the context of the transformed Eulerian mean approach (Andrews et al., 1987). The meridional and vertical components of the RMC can be calculated by the following formulas (Andrews et al., 1987; Butchart, 2014):

$$\overline{v}^* = \overline{v} - \rho^{-1}\frac{\partial}{\partial z}\left(\rho\frac{\overline{v'\theta'}}{\partial\overline{\theta}/\partial z}\right), \quad (1)$$

$$\overline{w}^* = \overline{w} + \frac{1}{a\cos\varphi}\frac{\partial}{\partial\varphi}\left(\frac{\cos\varphi\overline{v'\theta'}}{\partial\overline{\theta}/\partial z}\right), \quad (2)$$

where the overbars denote the zonal-mean values, the dashes mark the deviations of hydrodynamic quantities from their zonal-mean values; v and w are the meridional and vertical components of wind; ρ is background atmospheric density; z is vertical log-isobaric coordinate; θ is potential temperature; φ *is* latitude; a is the Earth’s radius.

Introducing deviations from the mean zonal components of the wind velocity and potential temperature as $v' = v - \overline{v}$; $\theta' = \theta - \overline{\theta}$ one can obtain the following equations used in this study for calculating the meridional and vertical components of the residual mean circulation from the wind and temperature fields simulated with the MUAM:

https://doi.org/10.5194/angeo-2020-71
Preprint. Discussion started: 23 October 2020

Annales Geophysicae Discussions
Open Access
EGU

$$\overline{v}^* = \overline{v} - \frac{1}{\partial\overline{\theta}/\partial z}\left(-\frac{\overline{v'\theta'}}{H} + \frac{\partial\overline{v'\theta'}}{\partial z} - \frac{\overline{v'\theta'}}{\partial\overline{\theta}/\partial z}\frac{\partial^2\overline{\theta}}{\partial z^2}\right), \quad (3)$$

$$\overline{w}^* = \overline{w} + \frac{1}{a\cos\varphi}\frac{1}{\partial\overline{\theta}/\partial z}\left(-\sin\varphi\overline{v'\theta'} + \cos\varphi\left(\frac{\partial\overline{v'\theta'}}{\partial\varphi} - \frac{\overline{v'\theta'}}{\partial\overline{\theta}/\partial z}\frac{\partial^2\overline{\theta}}{\partial z\partial\varphi}\right)\right). \quad (4)$$

In contrast to the conventional mean Eulerian circulation (having velocity components $\overline{v}$ and $\overline{w}$) the residual vertical velocity $\overline{w}^*$ is proportional to the rate of diabatic heating. It roughly represents a diabatic circulation in the meridional plane (Shepherd, 2007), i.e., when the heating of ascending air parcels and the cooling of descending air take place, while their potential temperature adapts to the local environment. Thus, the time-averaged RMC approximates the average movement of air masses and, therefore, it can be observed as the average movements of conservative gas components.

Figure 1 shows a comparison of RMC streamlines and wind vectors simulated with the MUAM (the top panels) and those obtained from the database of meteorological information reanalysis MERRA-2 (Gelaro et al., 2017) for the year 2010 (the bottom panels). The streamlines in the Figure 1a show two main RMC cells with an upwelling at low and middle latitudes of the Southern Hemisphere and downwelling at high latitudes of both hemispheres. The Eulerian mean meridional circulation in each hemisphere usually consists of tropical Hadley cells controlled by diabatic heating, eddy-induced mid-latitude Ferrell cells and polar cells generated by temperature gradients (e.g., Holton, 2004). In contrast to that, the residual circulation consists of two Hadley cells transporting air masses from low to high latitudes (Butchart, 2014), which are visible in Figure 1. At the same time, in winter (Northern) Hemisphere, the circulation cell is much wider than that in the Southern Hemisphere with higher residual meridional and vertical velocities shown in the Figure 1b.

Comparisons of Figure 1 top and bottom panels show a correspondence between the structure and magnitude of the simulated RMC and obtained using reanalysis data. Birner and Bönisch (2011) calculated the RMC based on the data from the Canadian Middle Atmosphere Model and obtained streamline distributions for January, which are similar to those shown in the Figure 1a. Eluszkevicz et al. (1996) analyzed the RMC using modelling and observations with the Microwave Limb Sounder onboard the Upper Atmosphere Research Satellite. They presented the distributions of the vertical and meridional wind components, which are consistent with our Figure 1. The RMC structure shown in Figure 1 is also in agreement with that obtained by Gille et al. (1987) and Kobayashi and Iwasaki (2016). The latter study presents the RMC fields for winter in the Northern Hemisphere obtained with the data from the Limb Infrared Monitor of the Stratosphere on the Nimbus-7 satellite and from the JRA-55 reanalysis data (Kobayashi et al., 2015).

4. Residual circulation at the different SW stages

In this section, we study the changes in RMC at an altitude of 0 – 100 km during different stages of the composite SW event (averaged over 19 model runs) simulated with the MUAM. In addition, we estimate changes in meridional fluxes such relatively conservative gas species as ozone caused by simulated changes in the RMC. Residual wind components are calculated applying Eq. (3) and (4) to the wind and temperature fields obtained with the MUAM. Then these characteristics are averaged over 19 model runs, separately, for 11-day intervals “before”, “during” and “after” SW (see section 2).

Figure 2a shows simulated with the MUAM distribution of the residual meridional and vertical velocities averaged over 11-day intervals before simulated SWs and over 19 model runs. Both Figures 2a correspond to the main cells of the RMC, general structure of which is consistent with that presented in Figure 1 according to the current knowledge (e.g., Tegtmeier et al., 2008). Downward flows at the MLT heights of the Northern Hemisphere and upward flows in the Southern one contribute to the warming of the atmosphere near the North Pole and cooling near the South Pole in January, which are caused by adiabatic temperature changes inside vertical moving atmospheric parcels.

https://doi.org/10.5194/angeo-2020-71
Preprint. Discussion started: 23 October 2020

Figures 2b and 2c represent changes in the residual velocity components during and after the composite SW relative to the distributions before the event in Figure 2a. The hypothesis of nonzero differences in Figures 2b and 2c could be verified with the statistical paired Student's t-test (e.g., Rice, 2006). At each latitude-height grid point the data in Figures 2b and 2c are averaged over 66×19 = 1254 individual differences (11 days with 4-hour outputs for 19 model runs). The paired Student's test gave statistical confidence of nonzero differences larger 95% for almost all values shown in Figures 2b and 2c except shaded regions.

The Figures 2b2 and 2c2 demonstrate signs generally opposite to signs of vertical velocity in Figure 2a2, which corresponds to general RMC weakening during and after the SW. However, at latitudes higher 30° N there are areas of enhancement of the downward velocity at an altitudes of 20 – 70 km. These changes correspond to changes in meridional residual velocity component sown in Figures 2b1 and 2c1, where negative differences in v^* are generally opposite to positive v^* in Figure 2a1. Therefore, during and after SW, RMC becomes weaker in almost all regions presented in Figures 2b and 2c. Enhanced downward residual flows at altitudes 20 – 60 km at high northern latitudes during SW in Figure 2b2 correspond to a layer with increased northward velocities at altitudes 50 – 70 km seen in Figure 2b1. Increased downward residual flows at high-latitudes in Figure 2b2 correspond to increased adiabatic heating of high-latitude northern stratosphere during SWs. Therefore, increasing RMC in the winter stratosphere and mesosphere may contribute to the formation of high-latitude SW events. Figures 2c1 and 2c2 show that increased RMC at altitudes 40 – 70 km may still exist up to 20 days after SW events. After simulated SW in Figures 2c, RMC in the Northern Hemisphere generally weakens. Similar weakening of the mean Eulerian global meridional circulation was shown in Figure 3 in the paper by Koval et al. (2019).

In the Southern Hemisphere, the main differences in RMC during and after simulated SWs demonstrated in Figures 2b and 2c exist at the MLT altitudes and have signs generally opposite to the respective velocities shown in Figures 2a before SWs. Absolute values of the differences at altitudes near 90 km are larger after SW (Figure 2b1) than those during SW (Figure 2b2). This determines weakening of the northward residual meridional velocity at altitudes 80 – 100 km in the mid-latitude Southern Hemisphere up to 25 – 30 % during the composite SW and up to 30 – 40 % after SWs compared to that before the warming event in Figure 2a1. Respective decreases in the upward residual velocity presented in Figures 2a2 and 2b2 are observed at altitudes 80 – 100 km in the Southern Hemisphere. These changes may be produced by general RMC weakening in the Northern Hemisphere during and after SW events, which can influence the entire global circulation. Hence, increased MLT differences shown in Figure 2b compared to ones in Figure 2c and may reflect time delay due to propagations of RMC changes caused by simulated SWs from in the Northern to the Southern Hemisphere. In addition, simulated RMC differences after SWs could be partly produced by seasonal changes in the global circulation, as far as time intervals after SW have 3-week time delay compared to respective intervals before SW.

A remarkable feature of RMC is increasing residual meridional velocity at altitudes 50 – 70 km during and after SWs as can be noted in Figures 2b1 and 2c1, which are associated with increasing downward residual vertical velocities at altitudes 20-60 km at the high-latitudes in the Northern Hemisphere (Figure 2b2) during SWs. One may assume that transformations of the Northern Polar Vortex during SWs may increase downward fluxes near the North Pole and increase northward drifts just above the SWs, which then can span to the Southern Hemisphere. Figure 2c2 shows destructions of the increased downward fluxes at altitudes 20 – 70 km near the North Pole after simulated SWs, while the zone of increased northward residual meridional velocities at altitudes 50 – 70 km demonstrated in Figure 2c1 still exist up to the Southern Hemisphere. This may confirm that changes in vertical motions at altitudes of winter SWs may produce RMC changes, which can remain in the middle atmosphere for a few weeks after simulated SW events.

Widely assumed reasons for the RMC changes during different SW phases could be changes in space-time structure of SPWs and the associated wave-mean zonal flow interactions. Gavrilov et al. (2018) showed that in the stratosphere below 50 km, amplitudes of SPW1 with zonal wavenumber m = 1 are increased before simulated SWs and decreased during the events, while changes in SPW2 amplitudes are opposite. Recently, several studies have been devoted to the analysis of the

https://doi.org/10.5194/angeo-2020-71
Preprint. Discussion started: 23 October 2020

peculiarities of the RMC formation and development during SW events. Using data from the reanalysis of meteorological information, Song and Chun (2016) considered the contributions of various terms of the transformed Eulerian equations of temperature and angular momentum to the RMC formation at different SSW stages. Bal et al. (2017) studied the changes in the RMC based on the analysis of 76 model SSWs and of 17 major SSWs selected from the Era Interim reanalysis data. In both studies mentioned above, it was confirmed that large-scale wave disturbances are the main driving force of the RMC due to the transfer of energy and angular momentum in the middle atmosphere and the MLT region. Laskar et al. (2019) showed a significant weakening (up to a reversal) of both the mean and residual meridional circulation at the MLT heights during SSW observed in winters 2009/10 and 2012/13, leading to significant temperature fluctuations in the stratosphere of both hemispheres, which correspond our results discussed above.

Increased downward residual vertical velocities at altitudes 20 – 60 km at high northern latitudes during SWs in Figure 2b1 correspond to the increased net downward mass flows and to increased adiabatic cooling rate in the heat balance equation of the model. This may help to heating the polar stratosphere. Therefore, changes in the RMC may influence the mechanisms of SW formation at high latitudes.

5. Residual fluxes of conservative gases.

Global atmospheric meridional circulation is the most important transport mechanism for atmospheric gas species (Fishman and Crutzen, 1978). Vertical transport of air particles under the influence of the residual circulation of the atmosphere produces fluxes of gas species, which could be important for the climate changes. In the present study, we made diagnostics of simulated RMC fluxes of gas species using the example of ozone, which for short time intervals may be considered as conservative gas at heights of the lower and middle atmosphere. The MUAM includes a 3D ozone distribution (Suvorova and Pogoreltsev, 2011, Suvorova et al., 2017), which takes into account long-term climatic longitudinal variability. This distribution was compared by Suvorova and Pogoreltsev (2011) with the ozone empirical model by Randel and Wu (2007) and with databases by Hassler et al. (2008) and Cionni et al. (2011). The meridional, F_x, and vertical, F_z, components of gas RMC fluxes are estimated by multiplying the gas concentration by the residual vertical and meridional velocities, respectively. Therefore, at each grid node, we have the following formulae for the components of RNC ozone fluxes:

$$F_i = N_{O3} v_i^*, \qquad N_{O3} = 10^{-6} \rho X_{O3} N_A / \rho_0, \tag{5}$$

where v^*_i are the zonal- and monthly-mean meridional (i=x) and vertical (i=z) residual velocity components, ρ_0 is the surface atmospheric density, X_{O3} is the zonal-mean ozone mixing ratio in *ppm*, N_A is the Avogadro number.

Figure 3a shows zonal-mean vertical component F_z of RMC ozone flux (shaded) averaged over 11-days time intervals before the composite SW. Illustrated by arrows in Figure 3a, vectors of average ozone fluxes correspond to RMC cells shown in Figure 2a. In the troposphere and stratosphere, Figure 3a2 shows tropical upwelling and extratropical downwelling. Winter cell of ozone transport is stronger than the southern one, which is consistent with Figure 1 and with theory (e.g. Holton et al., 2004). At altitudes above 50 km, RMC transport of conservative gas species from high latitudes of the summer hemisphere to high latitudes of the winter hemisphere dominates in Figure 3a1. These RMC cells can significantly contribute to the changes in concentrations of ozone and other gas species on both hemispheres.

Shading and arrows in Figures 3b and 3c show differences in the zonal-mean ozone fluxes between intervals during and after simulated SWs and intervals before respective SWs, which are averaged over 19 MUAM runs. In the troposphere and stratosphere, the signs of F_z differences (Figures 3b and 3c) are generally opposite to the respective F_z values presented in Figure 3a. Therefore, magnitudes of ozone fluxes become generally smaller during and after simulated SWs, which corresponds to the changes in RMC in Figures 2b and 2c. Maximum decreases in the vertical ozone flux are at high northern latitudes at altitudes 10 – 20 km during and after the SW (see Figure 3b2 and 3c2), which corresponds to the largest

https://doi.org/10.5194/angeo-2020-71
Preprint. Discussion started: 23 October 2020

increases in the residual vertical velocity in these regions in Figures 2b2 and 2c2. The weakening of residual vertical ozone fluxes at the middle and high latitudes of the winter hemisphere may reach 30% during simulated SWs and 30 – 40% after the events at the altitudes of the ozone layer maximum.

At the altitudes above 50 km in Figures 3b1 and 3b2, the arrows of vector differences in the RMC ozone fluxes are directed generally opposite to the respective flux vectors (Figure 3a1). During simulated SWs at high northern latitudes, increased downward and upward fluxes below and above altitude of about 60 km, enforce northward increments in ozone fluxes at altitudes 60 – 70 km in Figure 3b1, which enhance RMC at these altitudes. This corresponds to enhanced meridional winds at altitudes 50 – 70 km in Figure 2b1 discussed in section 4.

The results of our numerical simulations have shown that SW events may have significant impacts on the RMC and on associated residual ozone fluxes in the middle and upper atmosphere of both hemispheres. However, it should be noted that using of predefined ozone distributions in the model is acceptable for diagnostics of ozone residual fluxes only for relatively short time intervals. Simulating ozone concentrations and fluxes over long time intervals requires the use of interactive models that should include photochemical blocks.

6. Conclusion

In the present study, estimations of the mean residual meridional circulation are performed, using temperature and wind fields obtained from a set of numerical simulations of the atmospheric general circulation with the MUAM model. The focus is made on changes of the RMC and corresponding fluxes of conservative gas species at different stages of simulated SW events. To achieve sufficient statistical confidence, the results of numerical simulations have been averaged over 19-member ensembles of the MUAM runs. The test simulations showed similarities between the RMC simulated with the MUAM and that based on the observational data, also with results of other models.

The changes in the RMC at altitudes 0 – 100 km at different stages of the composite SW event are simulated. Before simulated SWs in the Northern Hemisphere, the RMC with northward meridional and downward vertical velocities is dominating in the middle and upper atmosphere. Downward flows are maximum at high latitudes. They may produce adiabatic heating of the polar stratosphere and contribute to SW formations. During and after the composite SW, general deceleration of downward vertical flows in the middle northern latitudes slow-down northward RMC in the most of analyzed altitude regions. Decreases in the residual meridional velocity at MLT heights may reach up to 30% in the Northern Hemisphere and up to 40 % in the Southern Hemisphere during and after simulated SWs. During the composite SW, increased downward flows at altitudes 20 – 70 km at high northern latitudes may enforce enhanced northward residual RMC at altitudes 50 – 70 km extending to the Southern Hemisphere. Increased adiabatic heating caused by these increased downward flows may help to the SW developments.

Diagnostics of residual fluxes of conservative gas species (like ozone) are performed and their changes at different stages of the composite SW are estimated. General weakening of ozone RMC fluxes at the middle latitudes of the Northern Hemisphere may reach 30% during SW and 30 – 40% after this event at the altitudes of stratospheric ozone layer maximum.

The approach used in this work within the framework of the transformed Eulerian mean circulation allows obtaining the residual wind components, which effectively take into account wave effects on transport of atmospheric quantities and gas species in the meridional plane.

Author contribution. AK developed software packages for calculating the RMC, provided general management of the studies and formed a draft of the article. AB and KD performed model simulations. TE compared the data obtained with reanalysis database. NG and AP supervised the setting of numerical experiments with the MUAM. OT participated in statistical data processing. AZ calculated and analyzed ozone fluxes. All participants took part in the preparation of the final version of the article.

https://doi.org/10.5194/angeo-2020-71
Preprint. Discussion started: 23 October 2020

Acknowledgements. Developing new programs for analyzing RMC based on ensembles of with the MUAM was supported by the Russian Science Foundation (grant #20-77-10006). Performing of numerical experiments and their analysis were supported by the Russian Foundation for Basic Research (grant #20-55-53039). In accordance with the statement 1296 of the Civil Code of the Russian Federation, the Russian State Hydrometeorological University (RSHU) has all rights on the MUAM code. To access and use the computer codes one should obtain a permission from the Rector of RSHU via the address 79, Voronezhskaya street, St. Petersburg, Russia, 192007, phone: 007 (812) 372-50-92. The authors can assist in obtaining the permission.

References

Andrews, D. G., and McIntyre, M. E.: Planetary waves in horizontal and vertical shear: The generalized Eliassen–Palm relation and the mean zonal acceleration, J. Atmos. Sci., 33, 2031–2048, 1976.

Andrews, D.G., Holton, J.R., Leovy, C.B.: Middle Atmosphere Dynamics, Academic Press, Orlando, FL. 1987.

Bal, S., Schimanke, S., Spangehl, T., and Cubasch, U.: Enhanced residual mean circulation during the evolution of split type sudden stratospheric warming in observations and model simulations, J. Earth Syst. Sci. 127:68 Indian Academy of Sciences https://doi.org/10.1007/s12040-018-0972-x, 2017.

Birner, T., Bönisch, H.: Residual circulation trajectories and transit times into the extratropical lowermost stratosphere, Atmos. Chem. Phys., 11, 817—827, doi 10.5194/acp-11-817-2011, 2011.

Brewer, A. W.: Evidence for a world circulation provided by measurements of helium and water vapour distribution in the stratosphere, Q. J. R. Meteorol. Soc., 75, 351–363, doi:10.1002/qj.49707532603, 1949.

Butchart, N.: The Brewer-Dobson circulation, Rev. Geophys., 52, 157—184, doi:10.1002/2013RG000448, 2014.

de la Camara, A., Abalos, M., Hitchcock, P.: Changes in Stratospheric Transport and Mixing During Sudden Stratospheric Warmings, Journal of Geophysical Research: Atmospheres 123(7), 3356–3373, doi: 10.1002/2017JD028007, 2018.

Dobson, G. M. B.: Origin and distribution of polyatomic molecules in the atmosphere, Proc. R. Soc., A236, 187–193, 1956.

Dobson, G. M. B., D. N. Harrison, and Lawrence J.: Measurements of the amount of ozone in the Earth's atmosphere and its relation to other geophysical conditions, Proc. R. Soc., A122, 456–486, 1929.

Charlton, A.J., Polvani, L.M.: A new look at stratospheric sudden warmings. Part I: Climatology and modelling benchmarks, J. Clim. 20, 449–469, 2007.

Charney, J. G., and Drazin, P. G.: Propagation of planetary-scale disturbances from the lower into the upper atmosphere, J. Geophys. Res. 66, 83–109, 1961.

Cionni, I., Eyring, V., Lamarque, J.F. et al.: Ozone database in support of CMIP5 simulations: Results and corresponding radiative forcing, Atmos. Chem. Phys. 11. 11267–11292, doi:10.5194/acp-11-11267-2011, 2011.

Eliassen, A., Palm, E.: On the transfer of energy in stationary mountain waves, Geophys. Norv. 22, 1—23, 1961.

Eluszkevicz, J., Crisp, D., Zurek, R., Elison, L. et al.: Residual circulation in the Stratosphere and lower Mesosphere as diagnosed from Microwave Limb Sounder Data, J. Atm. Sci. 53(2). 217—240, 1996.

Eyring, V., et al.: A Strategy for process-oriented validation of coupled chemistry-climate models, Bull. Am. Meteorol. Soc., 86, 1117–1133, doi:10.1175/BAMS-86-8-1117, 2005.

Fishman, J., Crutzen, P. J. The origin of ozone in the troposphere, Nature, 274, 855—857, 1978.

Fröhlich, K., Pogoreltsev, A., Jacobi, Ch.: Numerical simulation of tides, Rossby and Kelvin waves with the COMMA-LIM model, Advances in Space Research, 32, 863—868, 2003.

Fuller-Rowell, T., Wu, F., Akmaev, R., Fang, T.-W., Araujo-Pradere, E.: A whole atmosphere model simulation of the impact of a sudden stratospheric warming on thermosphere dynamics and electrodynamics, J. Geophys. Res., 115, A00G08, doi: 10.1029/2010JA015524, 2010.

https://doi.org/10.5194/angeo-2020-71
Preprint. Discussion started: 23 October 2020

Funke, B., Lopez-Puertas, M., Bermejo-Pantaleon, D., Garcia-Comas, M., Stiller, G.P., von Clarmann, T., Kiefer, M., Linden, A.: Evidence for dynamical coupling from the lower atmosphere to the thermosphere during a major stratospheric warming, Geophys. Res. Lett., 37, L13803, doi: 10.1029/2010GL043619, 2010.

Gavrilov, N.M., Koval, A.V., Pogoreltsev, A.I., Savenkova, E.N.: Simulating influences of QBO phases and orographic gravity wave forcing on planetary waves in the middle atmosphere, Earth Planets Space, 67(86), OI, 10.1186/s40623-015-0259-2, 2015.

Gavrilov, N.M., Koval, A.V., Pogoreltsev, A.I., Savenkova, E.N.: Simulating planetary wave propagation to the upper atmosphere during stratospheric warming events at different mountain wave scenarios, Advances in Space Research, 61, 7, 1819-1836. doi 10.1016/j.asr.2017.08.022, 2018.

Gavrilov, N.M., Pogoreltsev, A.I., Jacobi, Ch.: Numerical modeling of the effect of latitude-inhomogeneous gravity waves on the circulation of the middle atmosphere, Izv., Atmos. Ocean. Phys., 41(1), 9–18, 2005.

Gelaro, R., McCarty, W., Suárez, M. J., Todling, R. et al.: The Modern-Era Retrospective Analysis for Research and Applications, version 2 (MERRA-2), J. Climate. 30(14)., 5419—5454, doi: 10.1175/JCLI-D-16-0758.1, 2017.

Gerber, E. P., et al.: Assessing and understanding the impact of stratospheric dynamics and variability on the earth system, Bull. Am. Meteorol. Soc., 93, 845–859, doi:10.1175/BAMS-D-11-00145.1, 2012.

Gille, J. C., Lyjak, L. V., Smith, A.: The Global Residual Mean Circulation in the Middle Atmosphere for the Northern Winter Period, J. Atm. Sci., 44(10) 1437—1452, 1987.

Haynes, P.H., McIntyre, M. E., Shepherd, T. G., Marks, C. J., Shine, K. P.: On the “downward control” of extratropical diabatic circulations by eddy-induced mean zonal forces, J. Atmos. Sci. 48(4), 651−678, 1991.

Hassler, B., Bodeker, G.E., Dameris, M.: Technical Note: A new global database of trace gases and aerosols from multiple sources of high vertical resolution measurements, Atmos. Chem. Phys., 8, 5403–5421, 2008.

Holton, J. R.: An Introduction to Dynamic Meteorology, Fourth edition. Elsevier Academic Press., 2004.

Holton, J. R., Haynes, P. H., McIntyre, M. E., Douglas, A. R., Rood, R. B., Pfister, L.: Stratosphere-troposphere exchange, Rev. Geophys., 33, 403-439, 1995.

Iwasaki, T., Hamada, H., and Miyazaki, K.: Comparisons of Brewer-Dobson circulations diagnosed from reanalyses, J. Meteor. Soc. Japan, 87(6), 997–1006. doi: 10.2151/jmsj.87.997, 2009.

Kobayashi, C., Iwasaki, T.: Brewer-Dobson circulation diagnosed from JRA-55, Journal of Geophysical Research 121(4), 1493-1510, 2016.

Kobayashi, S., Ota, Y., & Harada, H.: The JRA-55 Reanalysis: General specifications and basic characteristics, Journal of the Meteorological Society of Japan, 93, 5–48. https://doi.org/10.2151/jmsj.2015-00, 2015.

Koval, A.V., Gavrilov, N.M., Pogoreltsev, A.I., Drobashevskaya, E.A.: Numerical simulation of the mean meridional circulation in the middle atmosphere at different phases of stratospheric warmings and mountain wave scenarios, Journal of Atmospheric and Solar-Terrestrial Physics, 183, 11-18, Doi: 10.1016/j.jastp.2018.12.012, 2019.

Koval, A.V., Gavrilov, N.M., Pogoreltsev, A.I., Savenkova, E.N.: Comparisons of planetary wave propagation to the upper atmosphere during stratospheric warming events at different QBO phases, J. Atmos. Solar-Terr. Phys.,171, 201—209, doi: 10.1016/j.jastp.2017.04.013, 2018.

Laskar, F.,I., McCormack, J.P., Chau, J.L., Pallamraju, Hoffmann, D.P., Singh, R.P.: Interhemispheric Meridional Circulation During Sudden Stratospheric Warming, Journal of Geophysical Research: Space Physics, 124(8), 7112-7122, 2019.

Laštovicka, J.: Forcing of the ionosphere by waves from below, J. Atmos. Sol.-Terr. Phys., 68(3), 479–497, 2006.

Li, Q, Graf, H-F, Giorgetta, M.A.: Stationary planetary wave propagation in Northern Hemisphere winter – climatological analysis of the refractive index, Atmos. Chem. Phys., 7, 183–200, 2007.

Lindzen, R. S.: Turbulence and stress owing to gravity wave and tidal breakdown, J. Geophys. Res., 86, 9707–9714, 1981.

https://doi.org/10.5194/angeo-2020-71
Preprint. Discussion started: 23 October 2020

Liu, H., Doornbos, E., Yamamoto, M., Ram, S.T.: Strong thermospheric cooling during the 2009 major stratosphere warming, Geophys. Res. Lett., 38, L12102, doi: 10.1029/2011GL047898, 2011.

McIntyre, M.E.: How well do we understand the dynamics of stratospheric warmings. J. Meterol. Soc. Japan., 60, 37-64, 1982.

Nath, D., Chen, W., Zelin, C., Pogoreltsev A.I., Wei, K.: Dynamics of 2013 Sudden Stratospheric Warming event and its impact on cold weather over Eurasia: Role of planetary wave reflection, Sci. Rep., 6, 24174, doi: 10.1038/srep24174, 2016.

Pawson, S., et al.: The GCM-Reality Intercomparison Project for SPARC (GRIPS): Scientific issues and initial results, Bull. Am. Meteorol. Soc., 81, 781–796, doi:10.1175/1520-0477(2000)081<0781:TGIPFS>2.3.CO;2, 2000.

Pogoreltsev, A.I., Vlasov, A.A., Froehlich, K., Jacobi, Ch.: Planetary waves in coupling the lower and upper atmosphere, J. Atmos. Solar-Terr. Phys., 69, 2083–2101, doi: 10.1016/j.jastp.2007.05.014, 2007.

Pogoreltsev, A. I., Kanukhina, A. Yu., Suvorova, E. V., Savenkova, E. N.: Variability of Planetary Waves as a Signature of Possible Climatic Changes, J. Atmos. Solar-Terr. Phys., 71, 1529-1539, doi:10.1016/j.jastp.2009.05.011, 2009.

Pogoreltsev, A.I., Savenkova, E.N., Pertsev, N.N.: Sudden stratopheric warmings: the role of normal atmospheric modes, Geomagnetism and Aeronomy, 54(3), 357–372, 2014.

Randel, W.J., Wu, F.: A stratospheric ozone profile data set for 1979-2005: Variability, trends, and comparisons with column ozone data, J. Geophys. Res., 112, D06313, doi:10.1079/2006JD007339, 2007.

Rice, J.A.: Mathematical statistics and data analysis (3rd edition), Pacific Grove. Duxbury Press, 603 p. ISBN-10: 0534399428, 2006.

Savenkova, E.N., Gavrilov, N.M., Pogoreltsev, A.I.: On statistical irregularity of stratospheric warming occurrence during northern winters, Journal of Atmospheric and Solar-Terrestrial Physics, 163, 14–22, doi: 10.1016/j.jastp.2017.06.007, 2017.

Seviour, W. J. M., N. Butchart, Hardiman, S.C.: The Brewer-Dobson circulation inferred from ERA-Interim, Q. J. R. Meteorol. Soc., 138, 878–888, doi:10.1002/qj.966, 2012.

Shepherd T. G.: Transport in the middle atmosphere, J. Meteor. Soc. Japan., 85B, 165—191, 2007.

Siskind, D.E., Eckermann, S.D., McCormack, J.P., Coy, L., Hoppel, K.W., Baker, N.L.: Case studies of the mesospheric response to recent minor, major and extended stratospheric warmings, J. Geophys. Res. 115, D00N03, doi: 10.1029/2010JD014114, 2010.

Song, B-G., Chun H-Y., Residual Mean Circulation and Temperature Changes during the Evolution of Stratospheric Sudden Warming Revealed in MERRA // Atmos. Chem. Phys. Discuss., doi:10.5194/acp-2016-729, 2016

SPARC CCMVal,: SPARC report on the evaluation of chemistry-climate models, in SPARC Report No. 5, WCRP-132, WMO/TD-No, edited by V. Eyring, T. G. Shepherd, and D. W. Waugh, 2010.

Sun, L., Robinson, W.A.: Downward influence of stratospheric final warming events in an idealized model, Geophys. Res. Lett., 36, L03819, doi: 10.1029/2008GL036624, 2009.

Suvorova, E.V., Pogoreltsev, A.I.: Modeling of nonmigrating tides in the middle atmosphere, Geomagmetizm and Aeronomy. 51(1), 105-115, 2011.

Suvorova E.N., Drobashevskaya E.A., and Pogoreltsev A.I.: Climatic three-dimensional ozone distribution model based on MERRA reanalysis data, Proceedings of the Russian State Hydrometeorological University (in russian), 49, 38-46, 2017.

Swinbank, R., O'Neill, A.: Stratosphere-troposphere assimilation system, Mon. Weather Rev., 122, 686–702, 1994.

Tao, M.C., Liu, Y., Zhang, Y. L.: Variation in Brewer–Dobson circulation during three sudden stratospheric major warming events in the 2000s, Adv. Atmos. Sci., 34(12), 1415–1425, doi:10.1007/s00376-017-6321-1, 2017.

Tegtmeier, S., K. Krüger, I. Wohltmann, K. Schoellhammer, Rex, M.: Variations of the residual circulation in the Northern Hemispheric winter, J. Geophys. Res., 113, D16109, doi:10.1029/2007JD009518, 2008.

Yigit, E., and Medvedev, A. S.: Heating and cooling of the thermo-sphere by internal gravity waves, Geophysical Research Letters, 36, L14807, https://doi.org/10.1029/2009GL038507, 2009.

https://doi.org/10.5194/angeo-2020-71
Preprint. Discussion started: 23 October 2020

Yuan, T., Thurairajah, B., She, C.-Y., Chandran, A., Collins, R.L., Krueger, D.A.: Wind and temperature response of midlatitude mesopause region to the 2009 sudden stratospheric warming, J. Geophys. Res., 117, D09114. doi: 10.1029/2011JD017142, 2012.

410

https://doi.org/10.5194/angeo-2020-71
Preprint. Discussion started: 23 October 2020

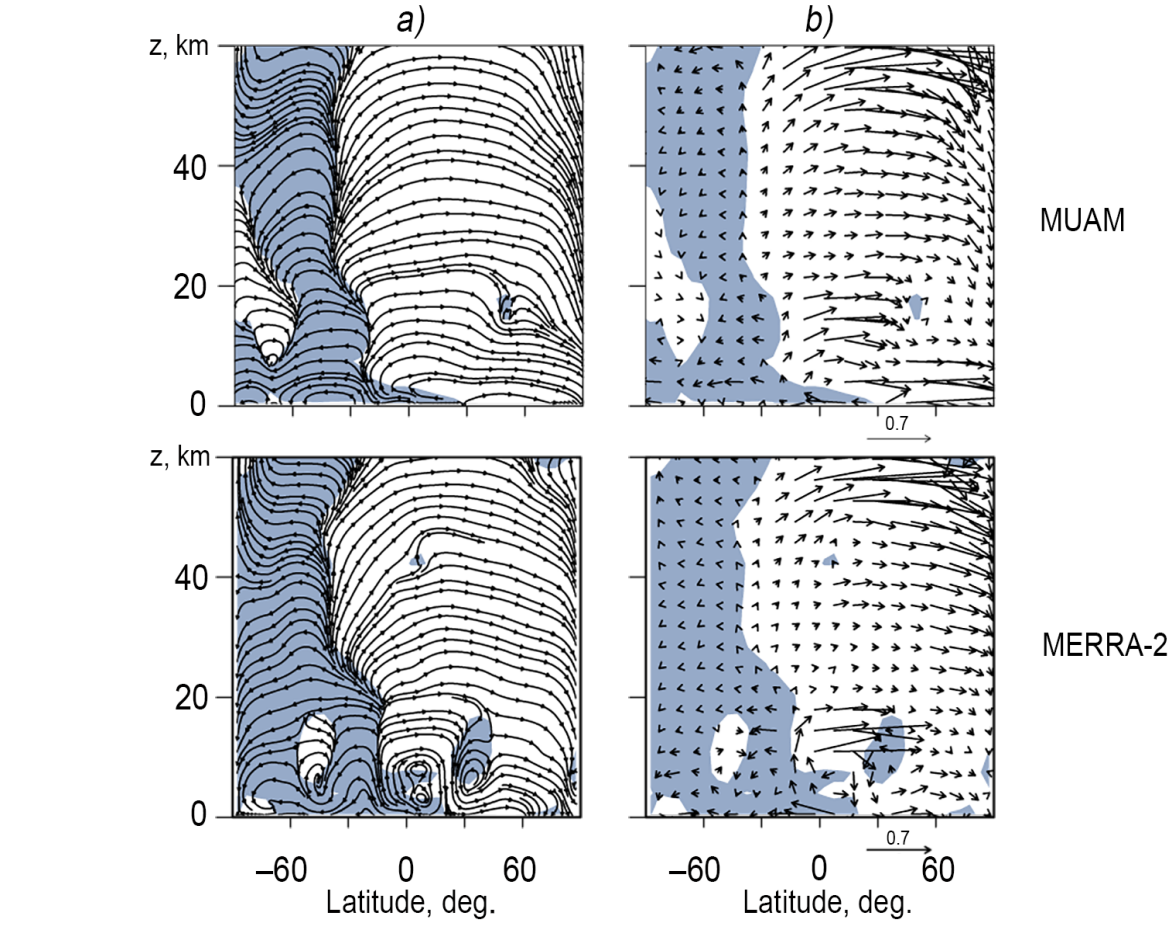

Figure 1: Latitude-altitude distributions of the RMC schematic streamlines (a) and wind vectors (b) averaged over 19 MUAM runs (top) and according to the MERRA-2 reanalysis data (bottom) for January. Areas with negative (southward) residual meridional wind are shaded with the gray-blue color. The streamlines and vectors are shown for the vertical velocity multiplied by factor 100.

https://doi.org/10.5194/angeo-2020-71
Preprint. Discussion started: 23 October 2020

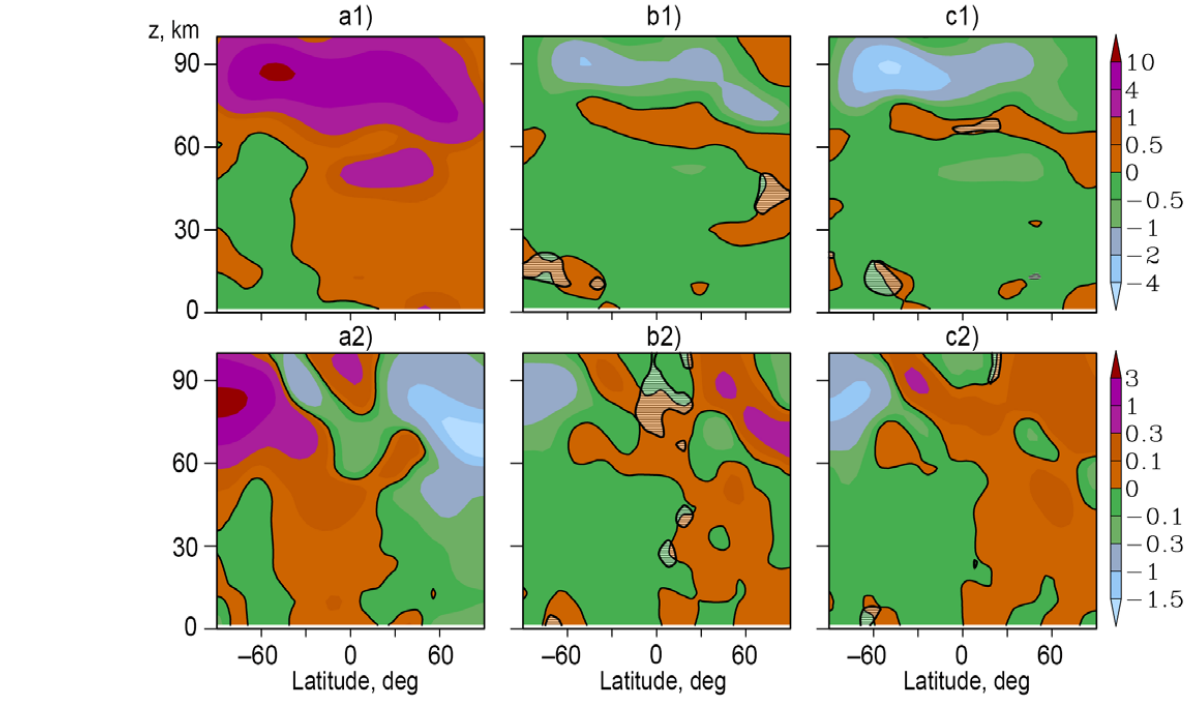

Figure 2: Zonal-mean residual meridional velocity in m/s (a1) and vertical velocity in cm/s (a2) averaged over 19 MUAM runs for 11-day intervals before SW; differences of respective values between the time intervals during and before SW (b), also after and before SW (c). Solid contours correspond to zero values. Shaded areas indicate regions of differences having significance less than 95% according to the paired t-test.

https://doi.org/10.5194/angeo-2020-71
Preprint. Discussion started: 23 October 2020

425

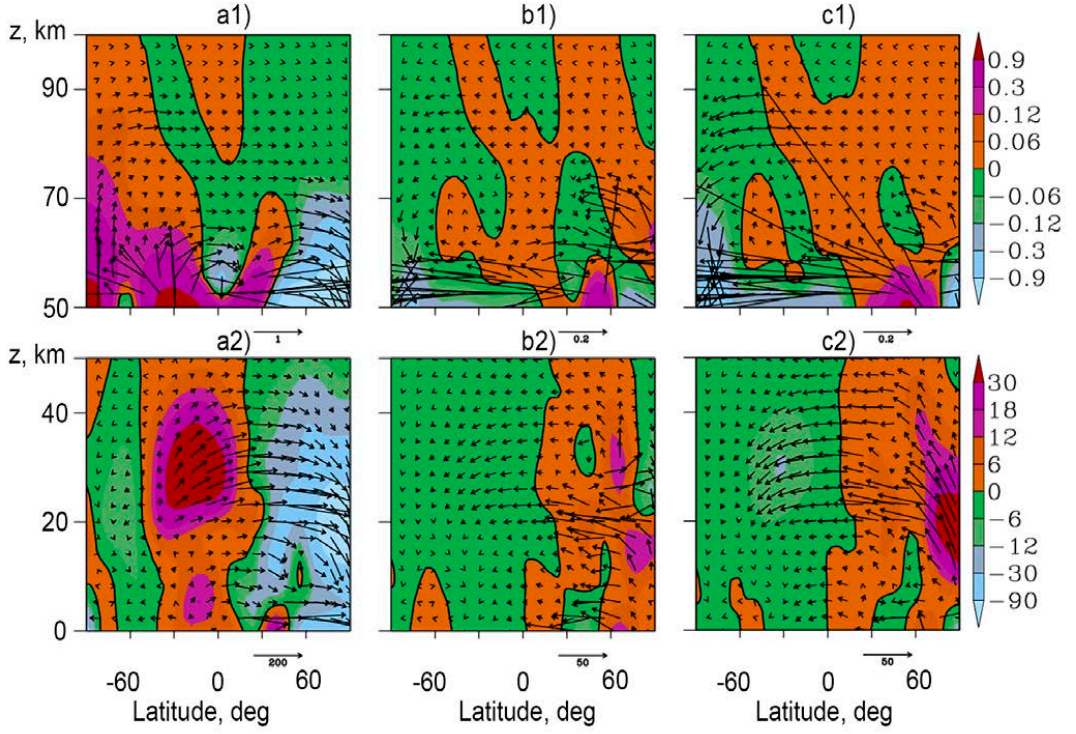

Figure 3: Zonal-mean vertical component of ozone RMC fluxes in 10^{14} $m^{-2}s^{-1}$ (shaded), averaged over time intervals before composite SW (a); its differences between intervals during and before SW (b) and after and before SW (c). Arrows show schematic vectors (with vertical velocity multiplied by factor 100) of the zonal-mean RMC ozone fluxes and their respective
430 differences. Solid contours correspond to zero values.